amcs

FAULT LOCATION IN EHV TRANSMISSION LINES USING ARTIFICIAL NEURAL NETWORKS

Tahar Bouthiba*

* University of Science and Technology of Oran
Faculty of Electrical Engineering
B.P. 1505 El-Mnaouar, Oran 31000, Algeria
e-mail: tbouthiba@yahoo.com

This paper deals with the application of artificial neural networks (ANNs) to fault detection and location in extra high voltage (EHV) transmission lines for high speed protection using terminal line data. The proposed neural fault detector and locator were trained using various sets of data available from a selected power network model and simulating different fault scenarios (fault types, fault locations, fault resistances and fault inception angles) and different power system data (source capacities, source voltages, source angles, time constants of the sources). Three fault locators are proposed and a comparative study of the proposed fault locators is carried out in order to determine which ANN fault locator structure leads to the best performance. The results show that artificial neural networks offer the possibility to be used for on-line fault detection and location in transmission lines and give satisfactory results.

Keywords: transmission line, fault detection, fault location, artificial neural networks

1. Introduction

An overhead transmission line is one of the main components in every electric power system. The transmission line is exposed to the environment and the possibility of experiencing faults on the transmission line is generally higher than that on other main components. Line faults are the most common faults, they may be triggered by lightning strokes, trees may fall across lines, fog and salt spray on dirty insulators may cause the insulator strings to flash over, and ice and snow loadings may cause insulator strings to fail mechanically. When a fault occurs on an electrical transmission line, it is very important to detect it and to find its location in order to make necessary repairs and to restore power as soon as possible. The time needed to determine the fault point along the line will affect the quality of the power delivery. Therefore, an accurate fault location on the line is an important requirement for a permanent fault. Pointing to a weak spot, it is also helpful for a transient fault, which may result from a marginally contaminated insulator, or a swaying or growing tree under the line.

Fault location in transmission lines has been a subject of interest for many years. During the last decade a number of fault location algorithms have been developed, including the steady-state phasor approach, the differential equation approach and the traveling-wave approach (Lian and Salama, 1994), as well as two-end (Sheng and Elan-

govan, 1998) and one-end (Zhang *et al.*, 1999) algorithms. In the last category, synchronized (Kezunovic and Mrkic, 1994) and non-synchronized (Novosel *et al.*, 1996) sampling techniques are used. However, two-terminal data are not widely available. From a practical viewpoint, it is desirable for equipment to use only one-terminal data. The one-end algorithms, in turn, utilize different assumptions to replace the remote end measurements. Most of fault locators are only based on local measurements. Currently, the most widely used method of overhead line fault location is to determine the apparent reactance of the line during the time that the fault current is flowing and to convert the ohmic result into a distance based on the parameters of the line. It is widely recognized that this method is subject to errors when the fault resistance is high and the line is fed from both ends, and when parallel circuits exist over only parts of the length of the faulty line.

Many successful applications of artificial neural networks (ANNs) to power systems have been demonstrated, including security assessment, load forecasting, control, etc. Recent applications in protection have covered fault diagnosis for electric power systems (Mohamed and Rao, 1995), transformer protection (Zaman and Rahman, 1998) and generator protection (Megahed and Malik, 1999). However, almost all of these applications in protection merely use the ANN ability of classification, that is, ANNs only output 1 or 0.

Various approaches have been published describing applications of ANNs to fault detection and location in transmission lines (Oleskovicz *et al.*, 2001; Purushothama *et al.*, 2001; Osowski and Salat, 2002). In this paper, a single-end fault detector and three fault locators are proposed for on-line applications using ANNs. A feedforward neural network based on the supervised backpropagation learning algorithm was used to implement the fault detector and locators. The neural fault detector and locators were trained and tested with a number of simulation cases by considering various fault conditions (fault types, fault locations, fault resistances and fault inception angles) and various power system data (source capacities, source voltages, source angles, time constants of the sources) in a selected network model.

2. Power System under Consideration

To evaluate the performance of the proposed neural network-based fault detector and locator, a 400 kV, 120 km transmission line extending between two sources as shown in Fig. 1 is considered in this study. The transmission line is represented by distributed parameters and the frequency dependence of the line parameters is taken into account.
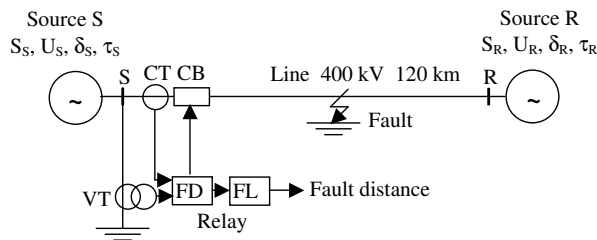

Fig. 1. System under study. VT: Voltage Transformer, CT: Current Transformer, CB: Circuit-Breaker, FD: Fault Detector, FL: Fault Locator.

The physical arrangement of the conductors is given in Fig. 2 and the conductor characteristics may be found in (Humpage *et al.*, 1982). A highly accurate transmission line simulation technique (Johns and Aggarwal, 1976) was utilized to generate voltage and current waveforms at the relay location (end S) for different fault types, fault conditions and different power system data.

3. Proposed Fault Detector and Locator Based on Neural Networks

Major functional blocks of the proposed fault detector and locator are shown in Fig. 3. Voltage and current signals at the transmission line end S (relay location) will be
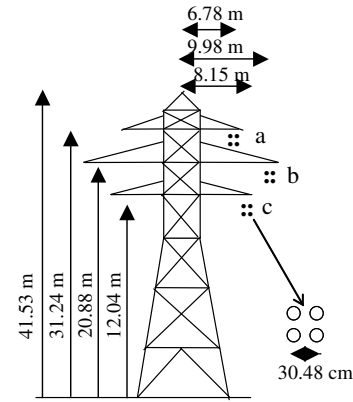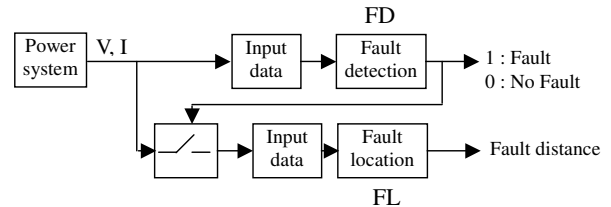

Fig. 2. Line configuration.

Fig. 3. Major blocks constituting the fault detector and locator.

acquired by the relay through CTs and VTs. After preprocessing, they will be fed to the fault detector (FD) to detect a fault, and if the fault is detected, the fault locator (FL) estimates the distance to the fault in the transmission line.

The proposed fault detector (FD) is designed to indicate the presence or absence of a fault. The occurrence of the fault is determined by identifying the power system state directly from instantaneous current (I) and voltage (V) data. The fault locator (FL) is designed to estimate the distance of the fault in the transmission line using the fundamental phasor magnitude of the voltage and current signals. The FD and the FL use only one terminal line datum extracted at the relay location (S).

4. Artificial Neural Networks and the Learning Algorithm

In this paper, the fully-connected multilayer feed-forward neural network (FFNN) was used and trained with a supervised learning algorithm called back-propagation. The FFNN consists of an input layer representing the input data to the network, some hidden layers and an output layer representing the response of the network. Each layer consists of a certain number of neurons; each neuron is connected to other neurons of the previous layer through adaptable synaptic weights w and biases b, cf. Fig. 4.
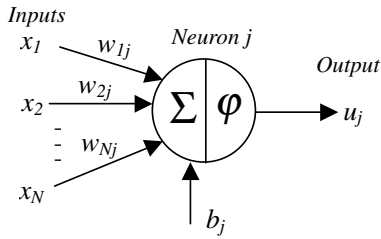
Fig. 4. Information processing in a neural network unit.

If the inputs of neuron j are the variables $x_1, x_2, \ldots, x_i, \ldots, x_N$, the output u_j of neuron j is obtained as follows:

$$u_j = \varphi \left(\sum_{i=1}^{N} w_{ij} x_i + b_j \right), \qquad (1)$$

where w_{ij} represents the weight of the connection between neuron j and the i-th input, b_j represents the bias of neuron j and φ is the transfer function (activation function) of neuron j.

An FFNN of three layers (one hidden layer) is considered with N, M and Q neurons for the input, hidden and output layers, respectively. The input patterns of the ANN represented by a vector of variables $x = (x_1, x_2, \ldots, x_i, \ldots, x_N)$ submitted to the ANN by the input layer are transferred to the hidden layer. Using the weight of the connection between the input and the hidden layer, and the bias of the hidden layer, the output vector $u = (u_1, u_2, \ldots, u_j, \ldots, u_M)$ of the hidden layer is then determined. The output u_j of neuron j is obtained as follows:

$$u_j = \varphi_{hid} \left(\sum_{i=1}^{N} w_{ij}^{hid} x_i + b_j^{hid} \right), \qquad (2)$$

where w_{ij}^{hid} represents the weight of connection between neuron j in the hidden layer and the i-th neuron of the input layer, b_j^{hid} represents the bias of neuron j and φ_{hid} is the activation function of the hidden layer.

The values of the vector u of the hidden layer are transferred to the output layer. Using the weight of the connection between the hidden and output layers and the bias of the output layer, the output vector $y = (y_1, y_2, \ldots, y_k, \ldots, y_Q)$ of the output layer is determined. The output y_k of neuron k (of the output layer) is obtained as follows:

$$y_k = \varphi_{out} \left(\sum_{j=1}^{M} w_{jk}^{out} u_j + b_k^{out} \right), \qquad (3)$$

where w_{jk}^{out} represents the weight of the connection between neuron k in the output layer and the j-th neuron

of the hidden layer, b_k^{out} represents the bias of neuron k and φ_{out} is the activation function of the output layer.

The output y_k (corresponding to the given input vector x) is compared with the desired output (target value) y_k^d. The error in the output layer between y_k and y_k^d ($y_k^d - y_k$) is minimized using the mean square error at the output layer (which is composed of Q output neurons), defined by

$$E = \frac{1}{2} \sum_{k=1}^{Q} (y_k^d - y_k)^2. \qquad (4)$$

Training is the process of adjusting connection weights w and biases b. In the first step, the network outputs and the difference between the actual (obtained) output and the desired (target) output (i.e., the error) is calculated for the initialized weights and biases (arbitrary values). During the second stage, the initialized weights in all links and biases in all neurons are adjusted to minimize the error by propagating the error backwards (the back-propagation algorithm). The network outputs and the error are calculated again with the adapted weights and biases, and the process (the training of the ANN) is repeated at each epoch until a satisfied output y_k (corresponding to the values of the input variables x) is obtained and the error is acceptably small.

The adjustment by the back-propagation algorithm (Bretas and Phadke, 2003), which is required in the weights and biases to minimize the total mean square error, is computed as

$$\Delta w = w^{new} - w^{old} = -\eta \frac{\partial E}{\partial w}, \qquad (5a)$$

$$\Delta b = b^{new} - b^{old} = -\eta \frac{\partial E}{\partial b}, \qquad (5b)$$

where η is the learning rate.

The computation in (5) reflects the generic rule used by the back-propagation algorithm. Equations (6) and (7) illustrate this generic rule of adjusting the weights and biases. For the output layer, we have

$$\Delta w_{jk}^{new} = \alpha \Delta w_{jk}^{old} + \eta \delta_k y_k, \qquad (6a)$$

$$\Delta b_k^{new} = \alpha \Delta b_k^{old} + \eta \delta_k, \qquad (6b)$$

where α is the momentum factor (a constant between 0 and 1) and $\delta_k = y_k^d - y_k$. For the hidden layer, we get

$$\Delta w_{ij}^{new} = \alpha \Delta w_{ij}^{old} + \eta \delta_j y_j, \qquad (7a)$$

$$\Delta b_j^{new} = \alpha \Delta b_j^{old} + \eta \delta_j, \qquad (7b)$$

where $\delta_j = \sum_k^Q \delta_k w_{jk}$ and $\delta_k = y_k^d - y_k$.

Once the network is trained with the algorithm and appropriate weights and biases are selected, they can be

used in the test to identify the output pattern given an appropriate input pattern. The training is performed off line resulting in reduced on-line computations.

5. Design Process of the ANN Fault Detector and the Fault Locator

The design process of the ANN fault detector and the fault locator goes through the following steps:

1. Preparation of a suitable training data set that represents cases the ANN needs to learn.

2. Selection of a suitable ANN structure for a given application.

3. Training the ANN.

4. Evaluation of the trained ANN using test patterns until its performance is satisfactory.

Tables 1 and 2 contain the parameter values used to generate data training sets and test patterns for the ANNs of the fault detector and the fault locator, respectively.

Table 1. Parameter settings for generating training patterns.

Fault location L_f (km)	3, 20, 40, ..., 100, 117
Fault inception angle θ_f (deg)	0, 45, 90
Fault resistance R_f (Ω)	0, 20, 40
Source capacities S_S, S_R (GVA)	9, 20
Source voltages U_S, U_R (pu)	0, 9, 1.1
Source angles δ_S, δ_R (deg)	$-20, 0, +20$
Time constants of the sources τ_S, τ_R (ms)	20, 80

Table 2. Parameter settings for generating test patterns.

Fault location L_f (km)	3, 4, 5, 6, ..., 116, 117
Fault inception angle θ_f (deg)	0, 30, 60, 90
Fault resistance R_f (Ω)	0, 5, 10, 30, 40
Source capacities S_S, S_R (GVA)	9, 10, 15, 20
Source voltages U_S, U_R (pu)	0.9, 1.0, 1.1
Source angles δ_S, δ_R (deg.)	$-20, -10, 0, +10, +20$
Time constants of the sources τ_S, τ_R (ms)	20, 50, 80

6. Fault Detector

6.1. Inputs and Outputs

In order to build up an ANN, the inputs and outputs of the neural network have to be defined for pattern recognition. The inputs to the network should provide a true representation of the situation under consideration. The process of generating input patterns to the ANN fault detector (FD) is depicted in Fig. 5.
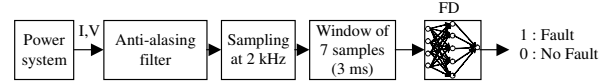

Fig. 5. Process for generating input patterns to the ANN fault detector.

The current (I) and voltage (V) signals are calculated as a string of samples corresponding to a 100 kHz sampling frequency. These signals are processed so as to simulate a 2 kHz sampling process (40 samples per 50 Hz cycle) using an anti-aliasing filter to remove the unwanted frequencies from a sampled waveform. This sampling rate is compatible with sampling rates presently used in digital relays.

The phase current (I_a, I_b, I_c) and voltage (V_a, V_b, V_c) signals, and the zero sequence current (I_0) and voltage (V_0) signals sampled at 2 kHz are used as the inputs to the ANN. It should be mentioned that the input current and voltage samples have to be normalized in order to reach the ANN input level (± 1). The ANN output is indexed with either a value of 1 (the presence of a fault) or 0 (the non-faulty situation).

6.2. Structure and Training of the Neural Fault Detector

The fault detection task can be formulated as a pattern classification problem. The fully connected three-layer feed-forward neural network (FFNN) was used to classify faulty/non-faulty data sets and the error back-propagation algorithm was used for training. The numbers of neurons in the input and hidden layers were selected empirically through extensive simulations. Various network configurations were trained and tested in order to establish an appropriate network with satisfactory performances, which were the fault tolerance, time response and generalization capabilities. Data strings of 7 consecutive samples of each signal sampled at 2 kHz are found to be appropriate inputs to the neural network as shown in Fig. 6. This represents a moving window with a length of 3 ms. In order to construct a good neural network system, it is vitally important to train and test it correctly. With supervised learning, the ANN is trained with various input patterns corresponding

to different types of fault (*a–g, b–g, c–g, a–b–g, a–c–g, b–c–g, a–b, a–c, b–c, a–b–c* and *a–b–c–g*, where *a*, *b*, and *c* are related to the phases and *g* refers to the ground) at various locations for different fault conditions (fault inception angles, fault resistances) and different power system data (source capacities, source voltages, source angles, time constants of the sources) as resumed in Table 1.
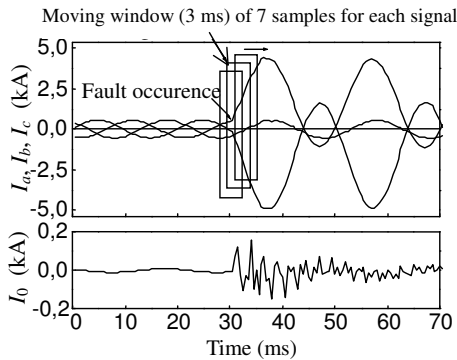

Fig. 6. Moving data window of seven samples used as the inputs to the ANN fault detector.

The ANN fault detector consists of 56 input neurons (seven samples of each signal: I_a, I_b, I_c, V_a, V_b, V_c, I_0, V_0), 18 neurons in the hidden layer (chosen after a series of trials) and one output neuron to indicate the transmission line state. Then the ANN structure of the fault detector is (56–18–1). The sigmoid transfer function

$$\varphi(S) = \frac{1}{1 + e^{-S}} \tag{8}$$

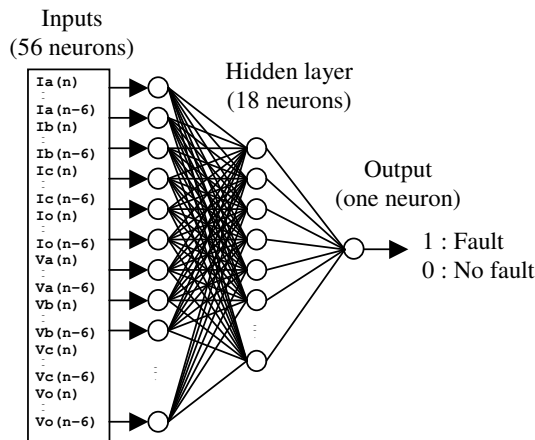was used for the hidden and output layers. The ANN structure of the fault detector is shown in Fig. 7.

The input layer simply transfers the input vector x (which are seven samples of each signal: $I_a(n), \ldots, I_a(n-6), I_b(n), \ldots, I_b(n-6), I_c(n), \ldots, I_c(n-6), I_0(n), \ldots, I_0(n-6), V_a(n), \ldots, V_a(n-6), V_b(n), \ldots, V_b(n-6), V_c(n), \ldots, V_c(n-6), V_0(n), \ldots, V_0(n-6))$ to the hidden neurons. The outputs u_j of the hidden layer with the sigmoid activation function are calculated in accordance with (2) and transferred to the output layer, which is composed of only one neuron. The output value of the neuron in the output layer with the sigmoid activation function calculated in accordance with (3) gives the state of the transmission line: 1 (the presence of a fault) or 0 (the non-faulty situation). It should be mentioned that the final weights and biases are adjusted by (7) in the training phase using the training parameters given in Table 1 with the same processing.

6.3. Tests and Results

After training, the neural fault detector was tested with 90 new fault conditions and different power system data for each type of fault are given in Table 2. Figures 8 to 11 show the phase current and voltage waveforms and the response of the proposed ANN fault detector for some fault conditions with power system data of $S_S = 10$ GVA, $U_S = 1\angle 20°$ pu, $\tau_S = 20$ ms and $S_R = 9$ GVA, $U_R = 0.9\angle 0°$ pu, $\tau_R = 50$ ms.

The results of Fig. 8 are obtained for a single phase to ground fault (*b–g*) with $L_f = 117$ km, $R_f = 5\,\Omega$ and $\theta_f = 30°$, which corresponds to the fault occurrence at time 27 ms. Figure 9 presents the results for a double phase to ground fault (*a–c–g*) with $L_f = 10$ km, $R_f = 40\,\Omega$ and $\theta_f = 90°$, which corresponds to the fault occurrence at time 30.5 ms.

The current and voltage waveforms and the ANN output shown in Fig. 10 are related to a double-phase fault
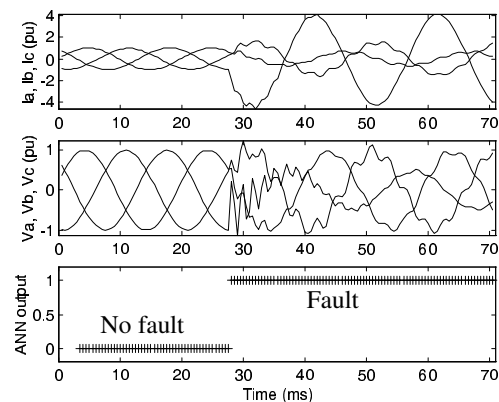

Fig. 7. ANN fault detector structure.

Fig. 8. Current and voltage waveforms and the ANN output for the *b–g* fault with $L_f = 117$ km, $R_f = 5\,\Omega$ and $\theta_f = 30°$.
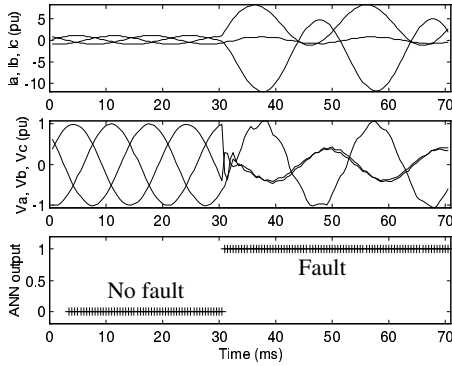
Fig. 9. Current and voltage waveforms and the ANN
output for the a–c–g fault with $L_f = 10\,\text{km}$,
$R_f = 40\,\Omega$ and $\theta_f = 90°$.

(b–c) with $L_f = 50\,\text{km}$, $R_f = 0\,\Omega$, and $\theta_f = 60°$, which corresponds to the fault occurrence at $29\,\text{ms}$.

Figure 11 shows the results for a three-phase to ground fault (a–b–c–g) with $L_f = 10\,\text{km}$, $R_f = 80\,\Omega$ and $\theta_f = 90°$, which corresponds to the occurrence of the fault at time $30.5\,\text{ms}$.
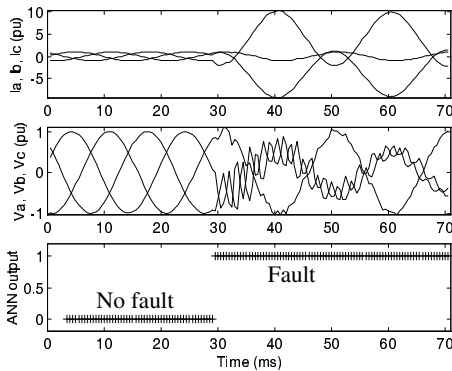

Fig. 10. Current and voltage waveforms and the ANN
output for the b–c fault with $L_f = 50\,\text{km}$,
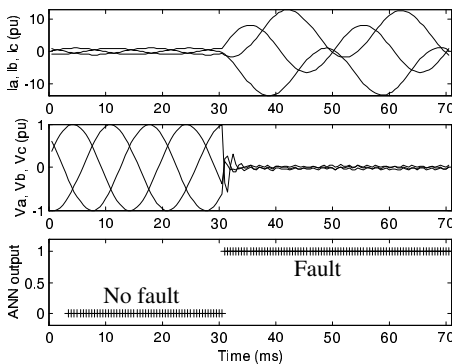$R_f = 0\,\Omega$ and $\theta_f = 60°$.

Fig. 11. Current and voltage waveforms and the ANN
output for the a–b–c–g fault with $L_f = 10\,\text{km}$, $R_f = 80\,\Omega$ and $\theta_f = 90°$.

The results demonstrate the ability of the fault detector to produce a correct response in all simulation tests. The results show the stability of the ANN outputs under normal steady-state conditions and rapid convergence of the output variables to the expected values (either very close to unity or zero) under fault conditions. This clearly confirms the effectiveness of the proposed fault detector. It should be mentioned that the technique described herein is based on a time domain moving window approach as discussed previously. The results show that in the fault cases presented, there is a very rapid transition in the ANN outputs as the windows move from the pre-fault to the fault states. The results reveal that the neural network is able to generalize the situation from the provided patterns, accurately indicates the presence or the absence of a fault and can be used for on-line fault detection.

6.4. Performance

The performance characteristics of the ANN fault detector are:

1. The stability of ANN output values in the normal steady-state and under fault conditions.

2. The minimal response time t_r of fault detection which is the difference between the desired fault detection time value t_d and the actual fault detection time value t_a:
$$t_r = t_a - t_d. \tag{9}$$

3. Generalization capabilities.

A good ANN fault detector is obtained when the response time is minimal, the ANN output values are stable in both the normal (e.g., 0) and fault (e.g., 1) conditions, and capable of providing fast and accurate fault detection in a variety of fault situations.

The only means of verifying the performance of a trained neural network is to perform extensive testing. After training, the neural fault detector is then extensively tested using independent data sets consisting of fault scenarios never used previously in training. As mentioned before, the fault detector performances are evaluated in terms of the response time t_r of the fault. The best performances are obtained when t_r is minimal.

Table 3 gives the percentage of fault cases versus the response time t_r for single phase to ground, double phase to ground, double phase, triple phase, triple phase to ground fault types and all faults. It can be seen that the maximum t_r is $1\,\text{ms}$. A number of 99.54% of fault cases are detected within a time of $0.5\,\text{ms}$ and a number of 0.45% of the tested cases are detected within a time of $1\,\text{ms}$. All faults (100%) are detected within a time of less than $1\,\text{ms}$, which indicates very good performance

for on-line fault detection. The obtained results are better than those in (Oleskovicz *et al.*, 2001).

Table 3. Fault cases versus the response time t_r for different fault types.

t_r [ms]	Number of fault cases (%)					
	Fault type					
	a–g b–g c–g	a–b–g b–c–g c–a–g	a–b b–c c–a	a–b–c	a–b–c–g	All faults
0.5	100	100	98.33	100	100	99.54
1.0	0.00	0.00	01.66	0.00	0.00	0.45

7. Fault Locator

7.1. Inputs and Outputs

The ANN fault locator (FL) is to locate faults in our transmission line. The FL is activated when a fault is detected by the fault detector (FD). The ANN forming the FL uses the magnitudes of the voltage and current phasors corresponding to the post-fault fundamental frequency (50 Hz) as inputs to the ANN. Most computer relays use the phasor representing the fundamental frequency of a signal sampled over a finite window, and the Fast Fourier Transform is the most common method to calculate the fundamental frequency phasor. Figure 12 shows the schematic
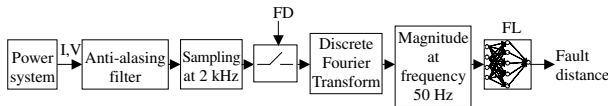

Fig. 12. Process for generating input patterns to the ANN fault locator.

diagram for the fault locator. The phase current and voltage signals extracted from the simulation at the relay location (end S) are processed (with an anti-aliasing filter) to simulate a 2 kHz sampling process (40 samples per one 50 Hz cycle). The one full cycle Discrete Fourier Transform (DFT) filter was utilized to obtain the magnitudes of the signals just after the fault occurrence and only the fundamental frequency component was used. In (Purushothama *et al.*, 2001) the authors use six cycles after the fault occurrence.

The magnitudes (only at the fundamental frequency of 50 Hz) of the three phase voltages ($|V_a|$, $|V_b|$, $|V_c|$) and phase currents ($|I_a|$, $|I_b|$, $|I_c|$) were used as the inputs of the neural network. It should be mentioned that the input variables have to be normalized in order to fit into the

ANN input range (± 1). The output of the ANN fault locator is the estimation of the fault location (in km) in the transmission line.

7.2. Structure and Learning Rule of the Neural Fault Locator

A three-layer feed-forward neural network (FFNN) trained using the back propagation algorithm was selected to implement the algorithm for fault location. In (Osowski and Salat, 2002) the authors use a hybrid neural network. As regards the ANN structure, parameters such as the number of inputs to the network as well as the neurons in the input and hidden layers were selected empirically. This process involved a trial-and-error procedure with various network configurations which were trained and tested in order to establish the appropriate network with a satisfactory performance. With supervised learning, the ANN was trained with various input patterns (cf. Table 1) corresponding to different types of fault at various locations for different fault conditions and different power system data. The transfer function of the hidden layer was the sigmoid function and that of the output layer neurons was the linear function

$$\varphi(S) = kS. \tag{10}$$

In this paper three fault locators are presented. The first (FL1) uses only current value magnitudes ($|I_a|$, $|I_b|$, $|I_c|$), the second (FL2) uses only voltage value magnitudes ($|V_a|$, $|V_b|$, $|V_c|$) and the third (FL3) uses both current and voltage value magnitudes (|Ia|, |Ib|, |Ic|, |Va|, |Vb|, |Vc|). The structure of each fault locator corresponds to the number of neurons in the input, hidden and output layers. The number of neurons in the input layer corresponds to the number of the input variables to the ANN. For FL1 and FL2 there are three neurons in the input layer and for the FL3 there are six neurons in the input layer. The number of neurons in the hidden layer was determined after a series of trials. It was found that eighteen neurons in the hidden layer for FL1 and FL2 and twenty neurons for FL3 lead to the best performance. The output layer consists of one neuron to estimate the fault location. So the ANN structures were 3–18–1, 3–18–1 and 6–20–1 for FL1, FL2 and FL3, respectively. The ANN structure of the FL3 is shown in Fig. 13.

The input layer simply transfers the input vector x (which is composed of the magnitudes of the currents and voltages at 50 Hz, i.e., $|I_a|$, $|I_b|$, $|I_c|$, $|V_a|$, $|V_b|$ and $|V_c|$) to the hidden neurons. The outputs u_j of the hidden layer with the sigmoid activation function were calculated in accordance with (2) and transferred to the output layer which consisted of only one neuron. The output value of the neuron in the output layer with the linear activation function,

calculated in accordance with (3), gives the fault location in the transmission line (in km). In the same way, the final weights and biases are adjusted in accordance with (7) in the training phase using the training parameters given in Table 1 with the same processing.

7.3. Test and Performance

In the following, we consider the fault classification (Bouthiba and Maun, 2003) and only the results for single-phase-to-ground faults (a–g, b–g, c–g) which represent the majority (85%) of the faults are presented. To get a good general performance, the fault locators were tested with a set of independent test patterns to cover wide system and fault conditions (fault inception angles, fault resistances) and different power system data (source capacities, source voltages, source angles, time constants of the sources) as given in Table 2.

Table 4 contains some test results for fault conditions ($R_f = 30\,\Omega$, $\theta_f = 90°$) and power system data ($S_S = 10\,\text{GVA}$, $U_S = 1\angle 20°$ pu, $\tau_S = 20\,\text{ms}$ and $S_R = 9\,\text{GVA}$, $U_R = 0.9\angle 0°$ pu, $\tau_R = 50\,\text{ms}$). The first column indicates the fault location and the three columns on the right indicate the outputs of the ANNs corresponding to the three fault locators FL1, FL2 and FL3, respectively.

The error in fault location is defined as

$$\text{Error (km)} = |\text{ANN output} - \text{Fault location}|, \quad (11)$$

where 'ANN output' is the output (in km) of the ANN fault locator and 'Fault location' is the real distance to the fault in the transmission line (in km).

Figures 14–16 show the error in the estimation of the fault location for FL1, FL2 and FL3, respectively.

The criterion for evaluating the performance of the fault locators is defined as

$$\text{Error (\%)} = \frac{|\text{ANN output} - \text{Fault location}|}{\text{length of the line}} 100\%. \quad (12)$$
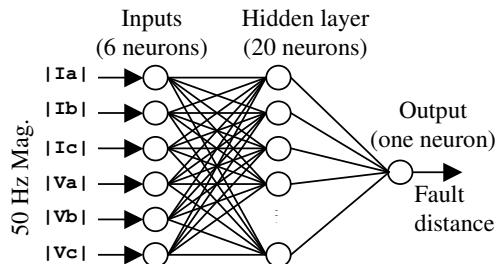
Table 4. Test results for fault location.

Fault location (km)	ANN output (km)		
	FL1	FL2	FL3
08.00	07.9519	08.0151	07.6660
13.00	13.0510	13.0400	12.7839
18.00	17.8848	17.9388	17.9528
23.00	22.8658	23.0389	23.1537
31.00	30.7401	30.7508	30.9293
42.00	42.1383	41.9349	41.9101
48.00	48.1432	47.9267	47.8919
58.00	57.7599	58.0352	57.8454
61.00	60.9604	61.2677	61.1975
72.00	71.8332	72.0497	72.1174
78.00	78.2810	77.9490	78.2182
83.00	82.8993	82.5490	82.7222
90.00	90.1776	90.0444	90.0219
95.00	94.9842	94.9412	94.8803
100.00	100.202	99.9474	100.004
105.00	105.073	105.270	105.177
110.00	110.015	110.568	110.306
115.00	114.795	114.429	114.804

Fig. 14. Test results of FL1.

Fig. 13. ANN structure of fault locator FL3.
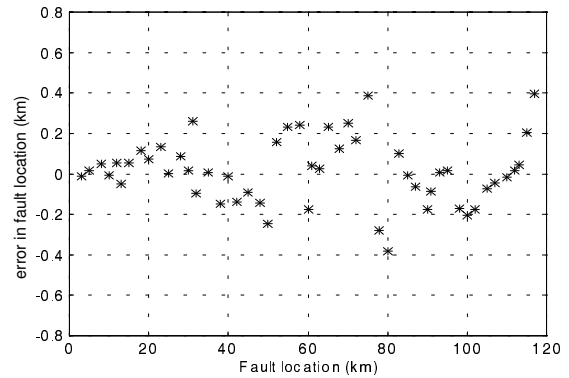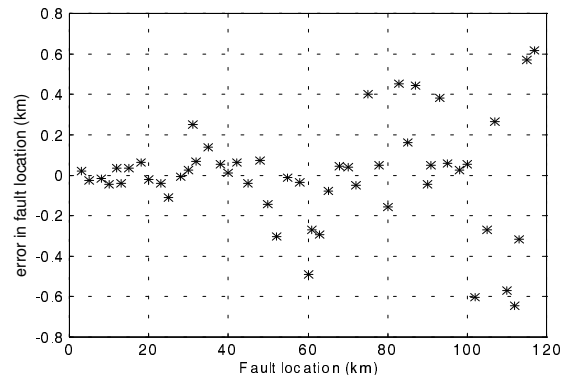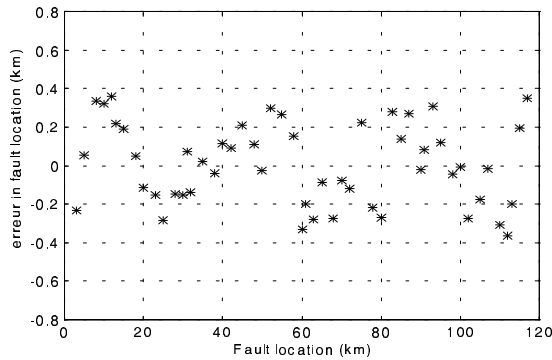

Fig. 15. Test results of FL2.

Fig. 16. Test results of FL3.

The minimum, maximum and average percentage errors of the fault locators are listed in Table 5 for all fault conditions and different power system data shown in Table 2. It can be seen that FL3, which uses current and voltage phasor magnitudes, is the best fault locator. The minimum error is 4.8 m (0.004%) and the maximum error is 364.7 m (0.3%), representing quite satisfactory results.

Table 5. Results of fault locators.

	Fault locator errors					
	FL1		FL2		FL3	
	(km)	(%)	(km)	(%)	(km)	(%)
Min.	0.0038	0.0031	0.0074	0.0062	0.0048	0.0040
Max.	0.3977	0.3314	0.6432	0.5360	0.3647	0.3039
Aver.	0.1215	0.1013	0.1743	0.1452	0.1803	0.1503

8. Conclusion

An efficient neural network-based fault detector for very fast EHV transmission line protection and three neural network-based fault locators have been proposed. The results demonstrated the ability of ANNs to generalize the situation from the provided patterns and to accurately indicate the presence and location of faults using only one terminal line datum. The neural fault detector uses only instantaneous current and voltage values, while the neural fault locator uses the magnitudes at the fundamental frequency of the voltage and/or current phasors. The presented test results demonstrate the effectiveness and the precision of fault detection in a variety of fault situations including fault types, fault locations, fault inception angles and fault resistances, and different power system data including source capacities, source voltages, source angles and source time constants. The ANNs thus have the possibility to be used for on-line fault detection and location in transmission lines .

References

Bouthiba T. and Maun J.C. (2003): *Relais à base de réseaux de neurones pour la protection des lignes de transport à THT*. — Revue Internationale de Génie Electrique, Vol. 6, No. 3–4, pp. 413–428.

Bretas A.S. and Phadke A.G. (2003): *Artificial neural networks in power system restoration*. — IEEE Trans. Power Delivery, Vol. 18, No. 4, pp. 1181–1186.

Humpage W.D., Wong K.P. and Nguyen T.T. (1982): *Network equivalents in power system electromagnetic transient analysis*. — Electric Power Syst. Res., Vol. 5, No. 3, pp. 231–243.

Johns A.T. and Aggarwal R.K. (1976): *Digital simulation of faulted e.h.v. transmission lines with particular reference to very high speed protection*. — IEE Proc. Generation, Transmission and Distribution, Vol. 123, No. 4, pp. 353–359.

Kezunovic M. and Mrkic J. (1994): *An accurate fault location algorithm using synchronized sampling*. — Electric Power Syst. Res., Vol. 29, No. 3, pp. 161–169.

Lian B. and Salama M.M.A. (1994): *An overview of digital fault location algorithms for power transmission lines using transient waveforms*. — Electric Power Syst. Res., Vol. 29, No. 1, pp. 17–25.

Megahed A.I. and Malik O.P. (1999): *An artificial neural network based digital differential protection scheme for synchronous generator stator winding protection*. — IEEE Trans. Power Delivery, Vol. 14, No. 1, pp. 130–138.

Mohamed E.A. and Rao N.D. (1995): *Artificial neural network based fault diagnostic system for electric power distribution feeders*. — Electric Power Syst. Res., Vol. 35, No. 1, pp. 1–10.

Novosel D., Hart D.G., Udren E. and Garitty J. (1996): *Unsynchronized two-terminal fault location estimation*. — IEEE Trans. Power Delivery, Vol. 11, No. 1, pp. 130–138.

Oleskovicz M., Coury D.V. and Aggarwal R.K. (2001): *A complete scheme for fault detection, classification and localisation in transmission lines using neural network*. — Proc. 7-th Int. Conf. *Developments in Power System Protection*, Amsterdam, the Netherlands, pp. 335–338.

Osowski S. and Salat R. (2002): *Fault location in transmission line using hybrid neural network*. — Compel, Vol. 21, No. 1, pp. 18–30.

Purushothama G.K, Narendranath A.U., Thukaram D. and Parthasarathy K. (2001): *ANN applications in fault locators*. — Electrical Power & Energy Syst., Vol. 23, No. 6, pp. 491–506.

Sheng L.B. and Elangovan S. (1998): *A fault location algorithm for transmission lines*. — Electric Machines & Power Syst., Vol. 26, No. 10, pp. 991–1005.

Zaman M.R. and Rahman M.A. (1998): *Experimental testing of artificial neural network based protection of power transformer*. — IEEE Trans. Power Delivery, Vol. 13, No. 2, pp. 510–515.

Zhang Q., Zhang Y., Song W. and Yu Y. (1999): *Transmission line fault location for phase-to-earth fault using one-terminal data*. — IEE Proc. Trans. Distribution., Vol. 146, No. 2, pp. 121–124.